Acta Mech
DOI 10.1007/s00707-014-1094-4

Vladimir S. Aslanov · Alexander S. Ledkov

Dynamics of towed large space debris taking into account atmospheric disturbance

Received: 17 January 2013 / Revised: 24 November 2013

Abstract The problem of deorbiting large space debris (SLD) by means of a tethered space tug is considered. A mathematical model that describes the plane motion of the system is developed. The model takes into account the effects of the atmosphere and the rotary motion of the SLD around the SLD center of mass. The effects of the moment of tension force, gravitational moment, and pitch moment on the SLD behavior are studied. The evolution of the phase space of an angle of attack during the SLD descent is considered. Singular points are found for special cases of motion. It is shown that the effect of the atmosphere on the SLD dynamics can be neglected above an altitude of 300 km. The situation that a tether becomes slack is observed. In this case, the SLD can oscillate with increasing amplitude and even pass into rotation. This is a dangerous situation that can lead to tether rupture. A method of thrust control that provides tension in the tether during the SLD deorbiting is presented. A slack tether is also observed at atmospheric entry. This phenomenon is caused by the difference in drag forces that act on the SLD and on the space tug. The obtained results can be used in the preparation of missions of space debris deorbiting.

Abbreviations

SLD	Large space debris
STS	Space tether system

1 Introduction

The problem of space debris has been extensively discussed in the scientific community in recent decades. The quantity of technogenic objects has been increasing steadily in near-Earth space, which has complicated putting new satellites into orbit and ensuring their safety. The issue is particularly acute in low orbits below an altitude of 2,000 km, and also for a geostationary orbit [1].

V. S. Aslanov (✉) · A. S. Ledkov
Theoretical Mechanics Department, Samara State Aerospace University, Samara, Russia
V. S. Aslanov
E-mail: aslanov_vs@mail.ru
URL: http://www.aslanov.ssau.ru
Tel.: +7-927-6889791

A. S. Ledkov
E-mail: ledkov@inbox.ru
URL: http://www.ledkov.com
Tel.:+7-909-3428886

Published online: 18 February 2014

Deorbiting of all new satellites after their missions are complete and of upper stages of new rockets is one measure that can be taken to stabilize the situation in the future. These operations should become an integral part of all new space programs. European experts estimate that such a measure can stop the growth of space debris [2,3]. However, the removal of new debris alone does not solve the problem since massive objects from previous missions that remain in orbit continue to be a danger. The modern evolutionary model of the motion of space debris shows that the debris population will grow as a result of collision and subsequent destruction of these objects even if no more rockets are launched [4].

Several projects of large space debris (SLD) removal are discussed in the literature. There are projects that use a high-power pulsed laser system for braking space objects and placing them on a descent trajectory [5,6]. Part of the work suggests using an active spacecraft (i.e., tug) that tows debris to a lower altitude. In this case, for its own safety, the tug is connected to the removed object without docking by an elastic tether or a special network [7,8]. There are projects in which debris is removed at the expense of the interaction of a conductive tether with the magnetic field of the Earth [9,10]. Many papers have investigated the dynamics of space tether systems (STSs) [11,12]. The control and stabilization of such a system upon tether deployment are important tasks for the considered problem of removing debris by towing [11,13].

A piece of space debris is considered as a point mass (material point) in existing papers [7–10]. This assumption is appropriate for the initial stages of study. Uncontrolled oscillations of the SLD can cause the tether to spin-up and rupture, and it is thus necessary to take into account the motion of the SLD around the SLD center of mass. Mathematical models of a space tether system that take into account the motion of one of the tip bodies around its center of mass have been presented [14,15]; however, these models consider the influence of the gravitational force only. The neglect of the atmosphere influence is a weak point of these studies.

The present study considers an STS that consists of an active spacecraft with a propulsion system called a space tug, a massless elastic tether, and a piece of SLD. The SLD is a rigid body. The tether provides the capture of the SLD and the transfer of a thrust force from the space tug to the SLD. The aim of this paper is to develop a mathematical model that describes the motion of the mechanical system taking into account the influence of the atmosphere and the gravitational moment and then to use the model in studying the SLD motion during towing.

The paper is divided into eight sections. Section 2 develops the mathematical model of the STS taking into account the influence of the atmosphere and the plane motion of the SLD around its center of mass. Section 3 describes a method of approximately calculating the aerodynamic characteristics, which are used in the mathematical model. Section 4 analyzes the effects of the aerodynamic and gravitational moments and the moment of the tension force, which act on the SLD during the descent. Section 5 investigates the phase portraits of the unperturbed motion of the SLD around its center of mass under the influence of various disturbing factors. Section 6 studies the motion of the system in the case that the tether can become slack and, as a result, the space tug and SLD start to move independently. In such cases, there can be an uncontrolled swing of the SLD and transition into rotation. A technique of thrust control, which provides tether tension throughout the descent, is offered in Sect. 7. Section 8 presents the numerical simulation of the SLD motion using the control.

2 Mathematical model

Let us study the plane motion of the STS. The SLD is considered as an axisymmetric rigid body with a center of mass at point C_2, and the space tug is considered as material point C_1 (Fig. 1). Tether fixing point P is on the axis of symmetry of the SLD. The STS moves in a central gravitational field. The space tug is equipped with a propulsion system that can provide constant thrust. We take into account the influence of the atmosphere on the space tug and the SLD. We use NRLMSISE-00 as a model of the atmosphere [16]. Earth's rotation is neglected.

The origin of the inertial coordinate system OXY coincides with the center of the Earth. Positions of the space tug and the SLD are determined by the distance to the center of the Earth r_i, the angle of the true anomaly ϑ_i, the flight-path angle γ_i, and the angle of attack α, where $i = 1$ corresponds to the space tug and $i = 2$ to the SLD (Fig. 1).

The equations of motion of the centers of mass C_1 and C_2 are [17]

$$m_i \dot{V}_i = -\frac{\mu m_i \sin\gamma_i}{r_i^2} - C_{\mathrm{Di}} A_i q_i - F_i \cos\gamma_i \\ -(2i-3)\frac{T}{l}\left(r_2 \sin\gamma_2 - r_1 \sin\left(\gamma_2 + \vartheta_2 - \vartheta_1\right)\right),$$

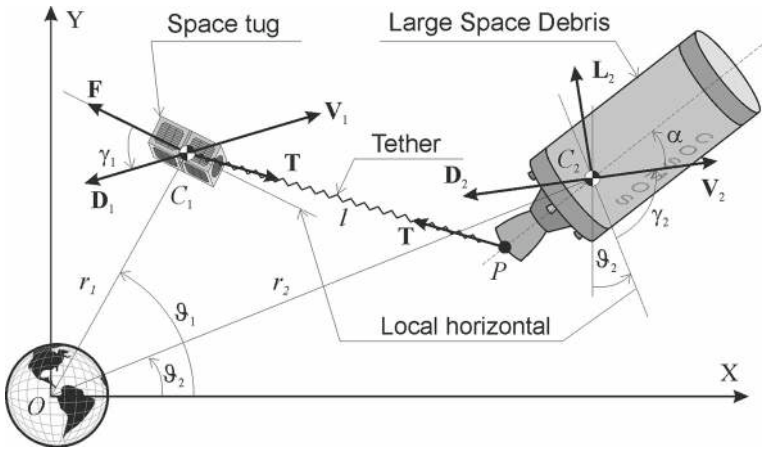

Fig. 1 Space tether system

$$
\begin{aligned}
m_i\dot{\gamma}_i &= -\frac{\mu m_i \cos\gamma_i}{r_i^2 V_i} + \frac{C_{\mathrm{Li}} A_i q_i}{V_i} + \frac{m_i V_i \cos\gamma_i}{r_i} + \frac{F_i}{V_i}\sin\gamma_i \\
&\quad -(2i-3)\frac{T_i}{l V_i}\left(r_2\cos\gamma_2 - r_1\cos\left(\gamma_2+\vartheta_2-\vartheta_1\right)\right), \\
\dot{\vartheta}_i &= -\frac{V_i\cos\gamma_i}{r_i}, \\
\dot{r}_i &= V_i\sin\gamma_i,
\end{aligned}
\tag{1}
$$

where V_i is the velocity of the ith point, μ is the gravitational parameter, $C_{\mathrm{Li}} = C_{\mathrm{Li}}(\alpha)$ is a dimensionless coefficient of the lift force, $C_{\mathrm{Di}} = C_{\mathrm{Di}}(\alpha)$ is a dimensionless coefficient of the drag force, $q_i = \rho(r_i)V_i^2/2$ is the dynamic pressure, $\rho(r)$ is the atmosphere density at a distance r from the center of the Earth, A_i is the area of the middle section of the ith body ($i = 1, 2$), $F_1 = F$ is the thrust, and $F_2 = 0$. $T = c\,(l - l_0)$ is the tension force, with c being the stiffness of the tether given by

$$
c = \begin{cases} ES/l_0, & \text{if } l \geq l_0, \\ 0, & \text{if } l < l_0, \end{cases}
\tag{2}
$$

where E is the modulus of elasticity of the tether, S is the area of the tether cross section, and l_0 is the length of the unstrained tether. l is the length of the tether (Fig. 1) given by

$$
l = \left[(r_2\cos\vartheta_2 - a\sin(\vartheta_2+\gamma_2+\alpha) - r_1\cos\vartheta_1)^2 + (r_2\sin\vartheta_2 - a\cos(\vartheta_2+\gamma_2+\alpha) - r_1\sin\vartheta_1)^2\right]^{1/2},
\tag{3}
$$

where $a = \mathrm{PC}_2$ is the distance from the center of mass of the SLD to the fixing point of the tether (Fig. 1). Note that the distance a is a few orders of magnitude less than r_2, and we can therefore write

$$
l^{-1} \approx \frac{1}{s} + \frac{r_2 a\sin(2\vartheta_2+\gamma_2+\alpha) - r_1 a\sin(\vartheta_2+\vartheta_1+\gamma_2+\alpha)}{s^3},
\tag{4}
$$

where $s = \sqrt{r_2^2 - 2r_1r_2\cos(\vartheta_1-\vartheta_2) + r_1^2}$. Equation (4) simplifies the equation of the system (1).

To obtain the equation of rotational motion of the SLD about its center of mass, we use the evolution equation for the angular momentum:

$$
\frac{\mathrm{d}K_2}{\mathrm{d}t} = M_\alpha + M_{\mathrm{T}} + M_{\mathrm{G}},
\tag{5}
$$

$$
M_\alpha = C_m A_2 L_2 q_2,
\tag{6}
$$

$$
M_{\mathrm{T}} = -\mathrm{ac}\,(l-l_0)\left(\frac{r_1}{l}\cos(\vartheta_2-\vartheta_1+\gamma_2+\alpha) - \frac{r_2}{l}\cos(\gamma_2+\alpha)\right),
\tag{7}
$$

$$
M_{\mathrm{G}} = -\frac{3\mu}{2r_2^3}(J_x - J_y)\sin(2\gamma_2+2\alpha),
\tag{8}
$$

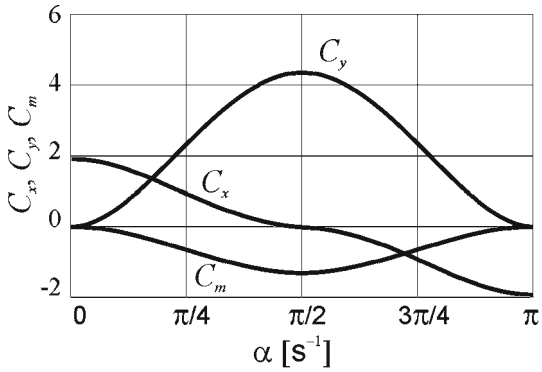

Fig. 2 Dependence of the aerodynamic coefficients on the angle of attack

where $K_2 = J_z(\dot{\vartheta}_2 + \dot{\gamma}_2 + \dot{\alpha})$ is the angular momentum of the SLD, t is time, J_z is the moment of inertia of the SLD, M_α is the pitching moment, $C_\mathrm{m} = C_\mathrm{m}(\alpha)$ is the coefficient of the pitching moment, L_2 is the characteristic size of the SLD, M_T is the moment of the tension force, and M_G is the gravitational moment [18].

From Eqs. (5)–(8), we have the equation of rotational motion of the SLD about its center of mass:

$$J_z(\ddot{\vartheta}_1 + \ddot{\alpha} + \ddot{\gamma}_2) = C_\mathrm{m} A_2 L_2 q_2 - \frac{3\mu}{2r_2^3}(J_x - J_y)\sin(2\gamma_2 + 2\alpha) - \mathrm{ac}\left(1 - \frac{l_0}{l}\right)(r_1\cos(\vartheta_2 - \vartheta_1 + \gamma_2 + \alpha) - r_2\cos(\gamma_2 + \alpha)). \tag{9}$$

3 Calculation of aerodynamic coefficients

To integrate Eqs. (1) and (9), it is necessary to know the values of the dimensionless aerodynamic coefficients $C_\mathrm{Di}(\alpha)$, $C_\mathrm{Li}(\alpha)$, and $C_\mathrm{m}(\alpha)$. Determination of the aerodynamic coefficients is a difficult task, and simplified calculation methods are thus used in practice. One widely applied technique is the shock theory of Newton, which provides simple results for the rarefied environment [19]. As a rule, the aerodynamics of a body are given by coefficients of the tangential and normal aerodynamic forces C_x and C_y, which are associated with C_D and C_L by the relations

$$\begin{aligned} C_D &= C_x\cos\alpha + C_y\sin\alpha, \\ C_L &= -C_x\sin\alpha + C_y\cos\alpha. \end{aligned} \tag{10}$$

In practice, it is convenient to expand these coefficients as Fourier series and to use only the first few terms in the expansions:

$$C_x = \sum_{j=1}^{N} c_{xj}\cos(j\alpha), \quad C_y = \sum_{j=1}^{N} c_{yj}\sin(j\alpha), \quad C_\mathrm{m} = \sum_{j=1}^{N} m_{zi}\sin(j\alpha). \tag{11}$$

As an example, let us consider the second stage of the space launch vehicle Cosmos 3M. This vehicle has delivered more than 300 satellites into orbit. As a result, at altitudes of 200–1,700 km, there is currently a large number of second stages of the Cosmos 3M [20]. When calculating the aerodynamics, we approximate the second stage of the Cosmos 3M as a cylinder with a flat bottom. The length of the cylinder is $L_\mathrm{c} = 6.5$ m, and the diameter is $D_\mathrm{c} = 2.4$ m. The mass of the stage is $m_2 = 1{,}500$ kg. The moments of inertia are $J_x = 1{,}285\,\mathrm{kg\,m^2}$, $J_y = 6{,}829\,\mathrm{kg\,m^2}$, and $J_z = 6{,}812\mathrm{kg\,m^2}$. The distance from the center of mass to the point of the tether attachment is $a = 4$ m [20]. Figure 2 presents graphs of the aerodynamic coefficients, which were obtained using Newton's method for the Cosmos 3M. Table 1 contains the coefficients of the Fourier series (11). The first three terms of the expansion (11) give good results for the considered body. In this case, the standard deviations are of the order of 10^{-3}.

Table 1 Coefficients in the expansions of aerodynamic coefficients

j (index of coefficient)	c_{xj}	c_{yj}	m_{zj}
1	1.5723	3.6131	−1.0569
2	−0.0012	0.0007	−0.0006
3	0.3145	−0.7226	0.2114
4	0	0	0
5	−0.0449	−0.1032	0.0302

4 Effect of moments on the descent trajectory

Accounting for the effects of the atmosphere severely complicates the equations of motion (1) and (9). At the same time, the density of the atmosphere at an altitude of 80 km is relatively low. This low density largely determines the long existence of space debris in orbit. The question of the appropriateness of the accounting of the effects of the atmosphere at high altitudes arises. The effects of various forces on the motion of the center of mass of a body in orbit have been assessed in the literature [21]. The motion of the SLD around the mass center is important for the considered problem. To estimate the magnitudes of the moments that define this motion, we carry out numerical simulation of the descent from a circular orbit at a height of 1,000 km to an altitude of 100 km. In the estimation, we consider the maximum possible amplitudes of the moments (6)–(8):

$$M_{\alpha\,\max} = \max(|C_{\mathrm{m}}|)A_2L_2q_2, \quad M_{\mathrm{T}\,\max} = \mathrm{ac}\max_{\mathrm{T}}(l-l_0)\,, \quad M_{\mathrm{G}\,\max} = \frac{3\mu}{2r_2^3}|J_x - J_y|,$$

where $\max\limits_{T}$ is the maximum value over the period of oscillation of the tether length $l(t)$. We assume that the tug mass is $m_1 = 500$ kg and that the tether has parameters $E = 1$ GPa, $l_0 = 1{,}000$ m, and diameter $d = 2$ mm.

The SLD and tug initially move in circular orbits (Fig. 1). The SLD is oriented along C_1C_2 (Fig. 1):

$$r_{i0} = 7{,}371\,\mathrm{km}, \quad V_{i0} = \sqrt{\mu/r_0}, \quad \gamma_{i0} = 0, \quad \vartheta_{10} = \pi/2. \tag{12}$$

The angle ϑ_2 can be found from the geometry:

$$\vartheta_{20} = -\arcsin\left(\frac{(l+a)^2 - 2r_{10}^2}{r_{10}^2}\right).$$

Initially, the length of the tether l is chosen so the modulus of projection of thrust F on the line C_1P equals the tension force T:

$$F\cos\beta = T = c(l - l_0),$$

where $\cos\beta = r_{20}\cos\vartheta_{20}(l+a)^{-1}$. Substituting here the expression for ϑ_{20}, we obtain the nonlinear equation for l, which can be solved numerically. We can then calculate values of ϑ_{20} and $\alpha_0 = \pi/2 - \vartheta_{20} - \beta$. We conduct a series of numerical calculations for different values of $F \in [0.1, 100]$N. The dependence of the time required for the SLD to descend to an altitude of 100 km on the thrust is shown in Fig. 3.

In the case that the force F lies on the designated border (0.1N $\le F \le$ 100N), at an altitude of 1,000 km, the inequality $M_{\alpha\,\max} < M_{\mathrm{G}\,\max} < M_{\mathrm{T}\,\max}$ holds. As the SDL altitude decreases, $M_{\mathrm{G}\,\max}$ and $M_{\alpha\,\max}$ increase. Figure 4 illustrates the relationship between the moments at different values of the force F. A gray area corresponds to the case that the tether is slack during the deorbiting. A white area corresponds to the case that the tether remains strained all the time.

During the initial stage of motion, the greatest impact on the SLD rotational motion is the moment of tension force M_{T}. The thrust F strongly affects this value. At an altitude of 1,000 km, $M_{\mathrm{T}\,\max}$ is two orders of magnitude greater than $M_{\mathrm{G}\,\max}$ for $F = 0.1N$. At higher values of F, this difference increases. The line $M_{\mathrm{T}\,\max} = 1{,}000M_{\alpha\,\max}$ divides Fig. 4 into two regions. The region above this line corresponds to the case when the moment of tension force is more than three orders of magnitude greater than the gravitational and pitching moments. Similarly, the region below the line $M_{\mathrm{G}\,\max} = 0.001\,M_{\alpha\,\max}$ (Fig. 4) corresponds to the case when the pitching moment is more than three orders of magnitude greater than the gravitational moment.

Thus, when motion occurs at heights greater than 300 km and the tether remains stretched all the time, the terms associated with aerodynamic and gravitational moments can be neglected in Eq. (9). If the tether is slack,

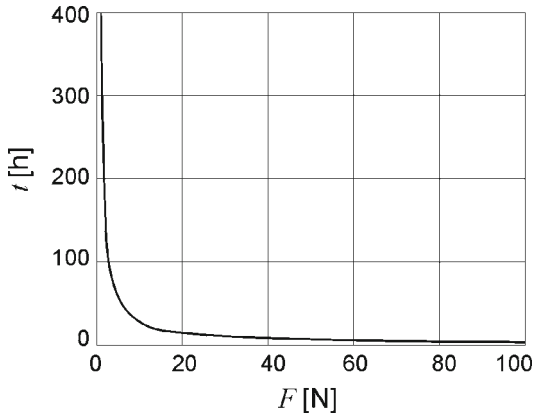

Fig. 3 Dependence of the time of descent on the thrust force

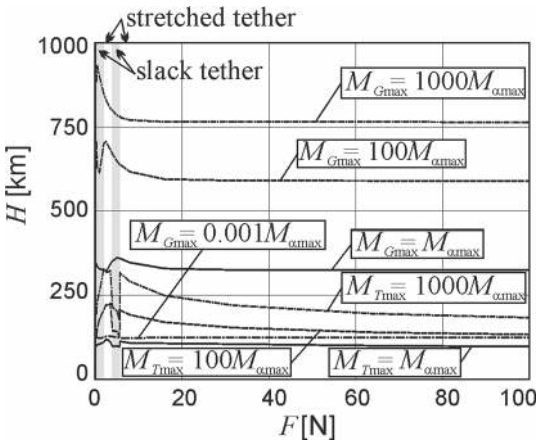

Fig. 4 Relationship between the moments at different values of F

at high altitudes, we can take into account only the gravitational moment (Fig. 4). At altitudes of 750–120 km, the gravitational and pitching moments should be taken into account. At altitudes lower than 120 km, we can take into account only the pitching moment.

5 Analysis of the SLD motion around the SLD center of mass

Motion around the mass center of a piece of debris that has large dimensions and a great mass strongly affects the motion of the system as a whole. Large amplitude oscillations or rotation of the SLD can lead to tangling and breakage of the tether. It is important to avoid such situations. To understand what types of motions the SLD can perform, we fix the parameters V_i, γ_i, ϑ_i and r_i and consider Eq. (9). The previous section showed that, at a certain altitude range, the motion of the SLD around its center of mass is determined by only the moment of the tension force, only the gravitational moment or only the pitching moment. We consider in detail these special cases and construct phase portraits and find singular points. This information will be used to illustrate the nature of spin-up of the SLD when the tether becomes slack.

5.1 General case

Let us choose a point on the descent trajectory, fix parameters V_i, γ_i, ϑ_i and r_i, and substitute Eq. (4) into Eq. (9):

$$\ddot{\alpha} + f(\alpha) = 0. \tag{13}$$

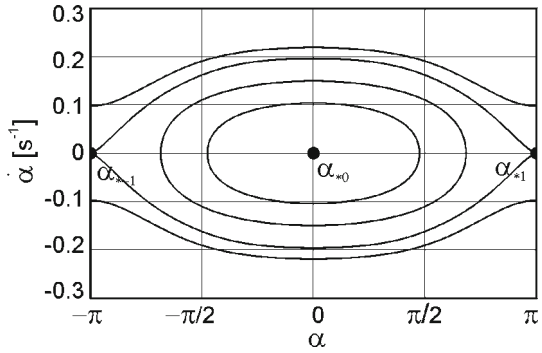

Fig. 5 Phase portrait of Eq. (15)

Equation (13) can be written as

$$\ddot{\alpha} + \sum_{j=0}^{3} (k_{cj} \cos j\alpha + k_{sj} \sin j\alpha) = 0, \tag{14}$$

where k_{cj} and k_{sj} are functions of the fixed parameters. Note that Eq. (14) has an energy integral

$$E = \frac{\dot{\alpha}^2}{2} + W(\alpha) = h = \text{const.},$$

where

$$W(\alpha) = \int \sum_{j=0}^{3} (k_{cj} \cos j\alpha + k_{sj} \sin j\alpha) \mathrm{d}\alpha = k_{c0}\alpha + \sum_{j=1}^{3} \left(\frac{k_{cj}}{j} \sin j\alpha - \frac{k_{sj}}{j} \cos j\alpha \right).$$

We consider particular cases that correspond to various points on the trajectory of the STS.

5.2 Motion under the action of the moment of the tether tension

If the motion occurs at high altitude, the moment of the tether tension determines the motion of the SLD. Numerical calculations showed that, at altitudes above 300 km, this moment surpasses the moments M_α and M_G by several orders of magnitude. In this case, some small terms in Eq. (13) can be neglected:

$$\ddot{\alpha} = -\frac{\mathrm{ac}\,(l - l_0)}{l J_z} \left(r_1 \cos(\gamma_2 + \alpha + \vartheta_2 - \vartheta_1) - r_2 \cos(\gamma_2 + \alpha) \right). \tag{15}$$

To find singular points, we make the right hand side of Eq. (15) equal to zero:

$$\alpha_{*k} = -\arctan \left(\frac{r_1 \cos(\vartheta_1 - \vartheta_2) - r_2}{r_1 \sin(\vartheta_1 - \vartheta_2)} \right) - \gamma_2 + \pi k, \quad k \in \mathbb{Z}. \tag{16}$$

Figure 5 shows an example of the phase portrait of the system in the case that the moment of the tether tension decisively determines the motion of the SLD.

On the phase portrait, two types of singular points are observed: saddles (when k is odd) and centers (when k is even). Heteroclinic trajectories connect saddle points [22]. There are areas of oscillation and rotation in the phase portrait. Oscillations can occur with large amplitude $\alpha_{\max} \in [0, \pi]$.

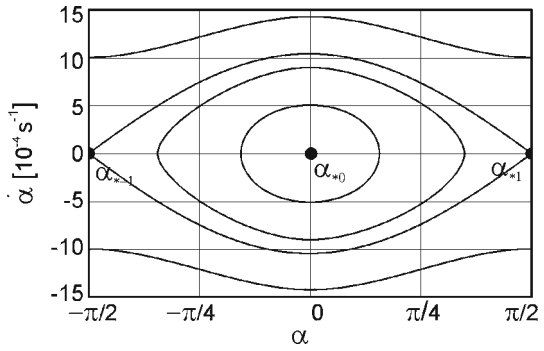

Fig. 6 Phase portrait of Eq. (18)

5.3 Motion under the action of the gravitational moment

When there is no tension force (i.e., $l < l_0$), according to Eq. (2), Eq. (13) takes the form

$$\ddot{\alpha} = \frac{q_2 A_2 L_2}{J_z} \sum_{j=1}^{3} (m_{zj} \sin j\alpha) - \frac{3\mu}{2r_2^3} \cdot \frac{J_x - J_y}{J_z} \sin(2\gamma_2 + 2\alpha). \tag{17}$$

The right hand side of the Eq. (17) contains two terms corresponding to the pitching and gravitational moments. Let us consider partial cases when one of these terms can be neglected.

At high altitudes, the density of the atmosphere is low and the gravitational moment decisively affects the motion of the SLD:

$$\ddot{\alpha} = -\frac{3\mu}{2r_2^3} \cdot \frac{J_x - J_y}{J_z} \sin(2\gamma_2 + 2\alpha). \tag{18}$$

In this case, the singular points α_{*k} are observed on a phase portrait (Fig. 6):

$$\alpha_{*k} = -\gamma_2 + \frac{\pi k}{2}, \quad k \in \mathbb{Z}.$$

Even values of k correspond to centers, and odd values to saddle points. Saddle points are connected by heteroclinic trajectories [22]. As in the previous case, there are areas of oscillations and rotation in the phase portrait, but in this case, the amplitude of the oscillations is less: $\alpha_{\max} \in \left[\frac{\pi k}{2}, \frac{\pi(k+1)}{2}\right], k \in \mathbb{Z}$.

5.4 Motion under the action of the pitching moment

When the influence of the gravitational moment is weak in comparison with the pitching moment, the motion of the SLD is approximately described by

$$\ddot{\alpha} = \frac{q_2 A_2 L_2}{J_z} \sum_{j=1}^{3} (m_{zj} \sin j\alpha). \tag{19}$$

This equation has singular points

$$\alpha_{*ck} = \pi k,$$
$$\alpha_{*sk} = (-1)^{(k)} \arccos\left(\frac{(-1)^{(k+1)} m_{z2} + \sqrt{m_{z2}^2 - 4m_{z3}m_{z1} + 4m_{z3}^2}}{4m_{z3}}\right) + \pi k, \quad k \in \mathbb{Z},$$

where m_{zj} are given in Table 1. If the expression under the operation of the arccos function is less than 1, then there are two types of singular points: α_{*ck} are centers and α_{*sk} are saddle points. In this case, there are

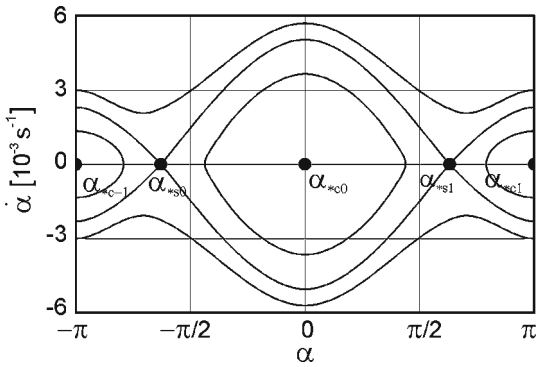

Fig. 7 Phase portrait of Eq. (19)

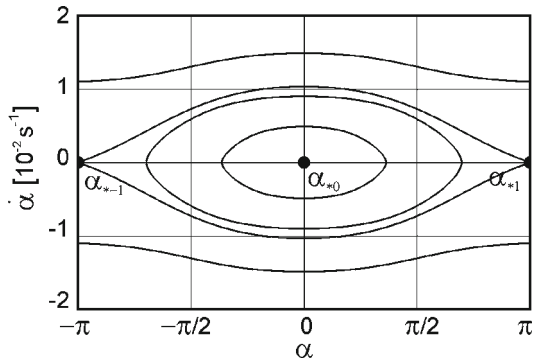

Fig. 8 Phase portrait of Eq. (19)

several oscillation areas of various sizes in the phase portrait (Fig. 7). If the expression under the operation of the arccos function is greater than 1, then there are singular points $\alpha_{*k} = \pi k$. Even values of k correspond to centers, and odd values to saddle points. Saddle points are connected by heteroclinic trajectories. The phase portrait is shown in Fig. 8. This case corresponds to the considered example of Cosmos 3M.

In all cases, there are areas in the phase portraits corresponding to oscillations and rotations. At the same time, the thicknesses of the areas covered by the separatrices differ by several orders of magnitude in the cases considered in Sects. 5.1, 5.2, and 5.3. In the next section, it will be shown that this is a prerequisite for the spin-up of the SLD.

6 Nature of the spin-up of the SLD

A series of numerical calculations showed that the considered STS is able to induce the descent of the SLD from an orbit. However, if the tether is initially slack, the distance between points P and C_1 periodically becomes less than l_0 during the descent. In this case, the tension force periodically disappears, and as a result, the SLD and tug start to move independently, the oscillations of the SLD cease to be regular, and the SLD may begin to rotate.

Figure 9 shows the change in the angle of attack with time obtained by numerical integration of the system of Eqs. (1) and (9) with initial conditions (12). Gray zones correspond to the free motion of STS elements, and white zones to the motion with the stretched tether. One can see that the SLD is first swinging and then transitions into rotation.

Let us consider the motion of the SLD in the case that the tension of the tether can disappear. If the tether is stretched, the moment of tension aspires to orient the SLD along a line that connects the centers of mass of the tug and SLD. Since there are no dissipative forces, the axis of the SLD continuously oscillates around this line. If at some time the tension force disappears, the SLD continues to rotate in the same direction owing to inertia. Comparing the phase portraits shown in Figs. 5 and 6, it is seen that the area of oscillations in the case of the stretched tether is much wider than that in the case of no tension force. In other words, upon the disappearance of tension force, the SLD remains in the area of oscillations if its angular velocity is very small. Otherwise,

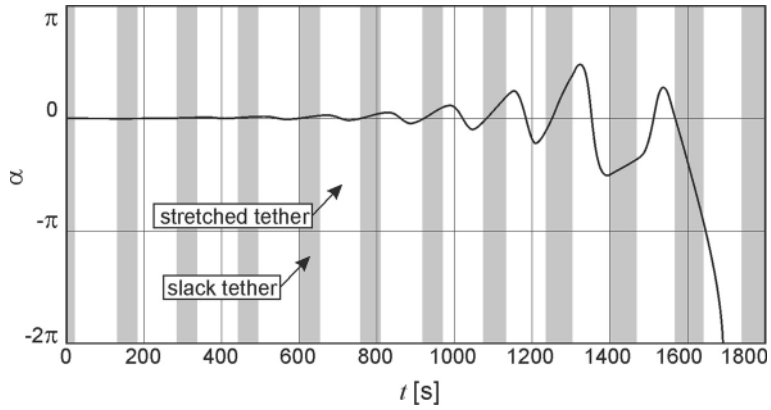

Fig. 9 Change in the angle of attack with time

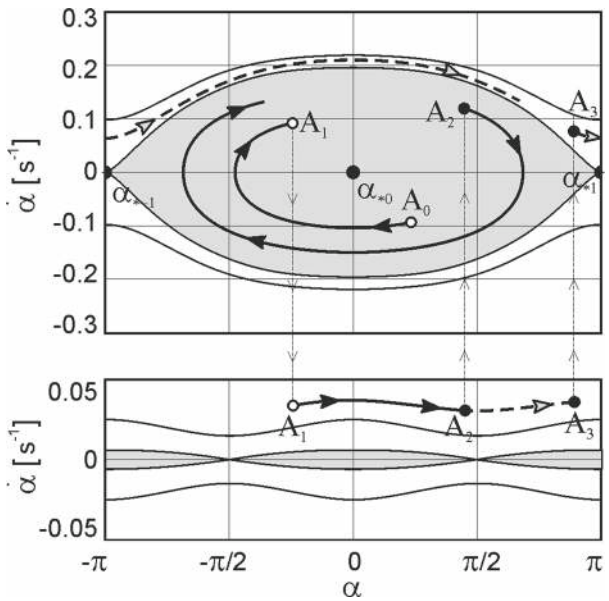

Fig. 10 Transition phase trajectories through the separatrix at the weakening of the tether (point A_1) and at re-tension (points A_2 and A_3); areas of oscillations bounded by separatrices are shown in *gray*

the SLD passes into rotation (point A_1 in Fig. 10). After a while, the tether stretches again. The representation point can either reenter the area of oscillations (point A_2 in Fig. 10) or stay in the field of rotation (point A_3 in Fig. 10). Thus, the presence of areas of free motion means that the phase trajectories can uncontrollably pass from one area bounded by the separatrix of phase space to another.

7 Thrust control for the tether tension

The situation that the tether is stretched at the moment of the engine switching on was considered in Sect. 4. In this case, oscillations of the SLD are regular. If the tether is initially slack, then no matter how great the thrust is, the tether will slacken again after a while. This situation was demonstrated in Sect. 6. Therefore, the problem of transferring the STS in a stretched condition and maintaining this state during descent is topical.

To study the longitudinal oscillation of the tether, we differentiate Eq. (3) twice and then substitute the second derivatives of Eqs. (1) and (13) into it. Since $l \gg a$, we assume that the parameter a is small and discard terms that contain it. We obtain the equation

$$\ddot{l} + f(l, \dot{l}) = 0.$$

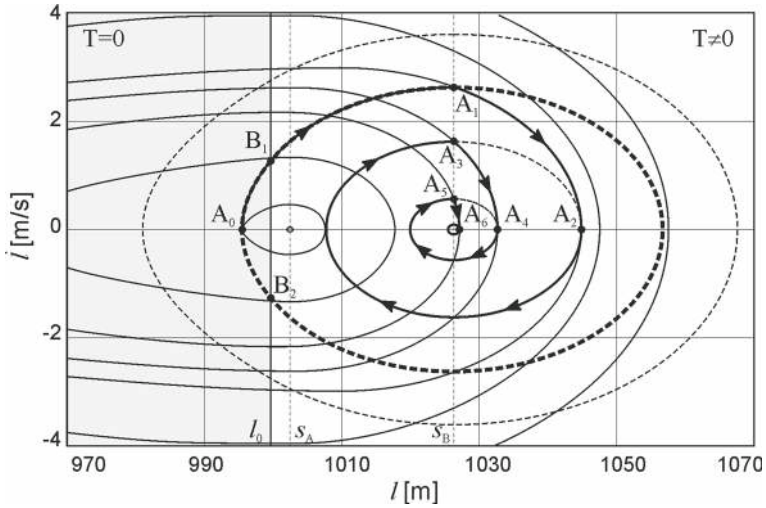

Fig. 11 Phase portrait; the *solid line* shows results for $F_\mathrm{A} = 10\,\mathrm{N}$ and the *dashed line* results for $F_\mathrm{A} = 100\,\mathrm{N}$

We fix a point on the descent trajectory (fixed parameters V_i, γ_i, ϑ_i and r_i) and consider the oscillations of the tether length.

The proposed principle of control is based on the fact that as the thrust increases, the tether length providing tension, which compensates this force, also increases. We assume that the engine of the space tug can operate in two modes, creating a constant thrust F_A or F_B ($F_\mathrm{B} > F_\mathrm{A}$). Let us consider the phase portrait $\dot{l}(l)$ shown in Fig. 11 and the corresponding graph of the deviation of the length of the tether from the balance position (Fig. 12). The thin solid lines correspond to thrust F_A and dashed lines to thrust F_B. Figure 11 illustrates that the increase in thrust leads to a shift in the singular point to the right. The point s_A corresponds to thrust F_A and the point s_B to thrust F_B. The area to the left of the vertical line $l = l_0$ corresponds to the motion of the STS with a slack tether. To the right of this line, there is a zone where the motion of the system is affected by the tension force.

We suppose that the tether is initially slack, and the system is at point A_0 (Figs. 11, 12). After switching on the constant thrust F_B, the representative point will move along the phase trajectory shown by the thick dashed line in the figure. The tether will be stretched at point B_1 but slack again some time later at point B_2. The purpose of the control is transfer of a representative point in a neighborhood of the equilibrium position s_B by the thrust switching on and off.

To translate the representative point on a trajectory located closer to the equilibrium position, it is necessary to switch the thrust to F_A at the point $l = s_\mathrm{B}, \dot{l} > 0$ (point A_1). The representative point moves on a trajectory around s_A. This trajectory passes closer to the point s_B than the initial trajectory. The thrust switches back to F_B when the representative point reaches the straight line $\dot{l} = 0$ (point A_2). The described process can be repeated multiple times, while the representative point does not appear at the required distance from s_B.

8 Dynamics of the controlled motion of the STS

We simulate the descent of the SLD using the principle of control described in Sect. 7. We consider the STS with the parameters specified in Sect. 4. Initially, the tether is slack, and the distance between points P and C_1 is 980 m. The axis of the SLD deviates from the local vertical by an angle of $\pi/12$. Calculations show that up until entry into the atmosphere, the tether remains stretched and the angle of attack remains limited.

Figure 13 shows the change in height of the SLD with time and phase portraits that correspond to different points of the descent trajectory. The phase portraits are obtained using Eq. (13) for constant V_i, γ_i, ϑ_i, and r_i. Figure 13 shows that, in the process of height reduction, there is a displacement of the singular points (16) to the right. This effect is caused by reduction in the angle γ_2 with decreasing SLD altitude. From $t = 9{,}154\,\mathrm{s}$ ($H = 104\,\mathrm{km}$), the aerodynamic moment exceeds the moment of the tether's tension. At $t = 9{,}221\,\mathrm{s}$($H = 88\,\mathrm{km}$), the tether becomes slack and the motion of the SLD around the center of mass is defined by the influence of the pitching moment.

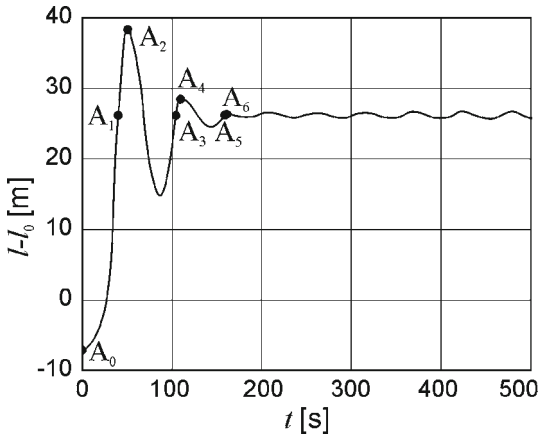

Fig. 12 Deflection of the tether's length from position l_0

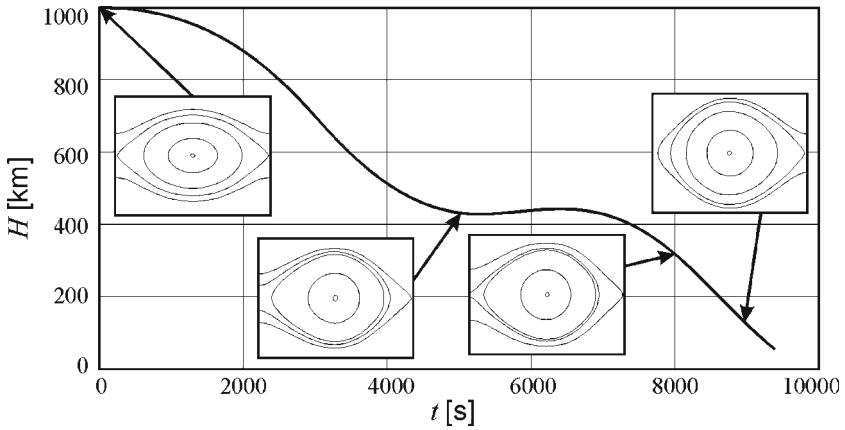

Fig. 13 Phase portraits in various points of a trajectory

The tether slack in the final stage is caused by the difference in the drag forces acting on the SLD and on the tug. The area of the cross section of the SLD surpasses the area of the tug's cross section, and the SLD is therefore decelerated by the atmosphere more quickly than the tug. As a result, the tug starts to catch up with the SLD and the tether tension disappears. To prevent this situation, it is possible to place an inflatable balloon in the tug. The balloon would provide a large cross section and allow effective braking of the tug by the atmosphere.

9 Conclusion

This study investigated a system that involves three elements: an active space tug as a mass point, an elastic tether, and a large piece of debris as a rigid body. The simulation results show that the large debris significantly affects the motion of the whole system. The motion of the space debris can lead to the tangling or rupture of the connecting tether. The effect of the atmosphere can be neglected above an altitude of 300 km. As a result of the aerodynamic force and moment and the thrust and gravitational torque, two modes for the tether are observed: strained and slack. In the case of a slack tether, the SLD may begin to oscillate with increasing amplitude and even pass into rotation. The SLD rotation is a dangerous situation, which can lead to tether rupture. A method of thrust control, which provides a tension of the tether during the SLD deorbiting, is presented. Note also that the slack tether is observed at atmospheric entry. This phenomenon is caused by the difference in drag forces acting on the SLD and on the space tug. Further studies are needed to determine whether these findings can be applied to actual system components.

Acknowledgments This work is funded by the Russian Foundation for Basic Research, Project No. 12-01-00317-a, 12-01-31114-mol_a.

References

1. Andrenucci, M., Pergola, P., Ruggiero, A.: Active Removal of Space Debris. Expanding foam application for active debris removal: final report. University of Pisa, Pisa (2011). http://www.academia.edu/776966/Active_Removal_of_Space_Debris_-_Expanding_foam_application_for_active_debris_removal
2. Klinkrad, H., Beltrami, P., Hauptmann, S., Martin, C., Sdunnus, H., Stokes, H., Walker, R., Wilkinson, J.: The ESA space debris mitigation handbook 2002. Adv. Space Res. **34**, 1251–1259 (2004)
3. GOST R 52925-2008 Space technology: General requirements for space systems to limit technogenic pollution of circumterrestrial space (National Standard of Russian Federation). Standard form. Moscow (2008) (in Russian)
4. Lewis, H.G., White, A.E., Crowther, R., Stokes, H.: Synergy of debris mitigation and removal. Acta Astronaut. **81**, 62–68 (2012)
5. Campbell, J.W.: Using Lasers in Space: Laser Orbital Debris Removal and Asteroid Deflection. Air University, Maxwell Air Force Base, Alabama (2000)
6. Phipps, C.R., Baker, K.L., Libby, S.B., Liedahl, D.A., Olivier, S.S., Pleasance, L.D., Rubenchik, A., Trebes, J.E., George, E.V., Marcovici, B., Reilly, J.P., Valley, M.T.: Removing orbital debris with lasers. Adv. Space Res. **49**, 1283–1300 (2012)
7. Jasper, L.E.Z., Seubert, C.R., Schaub, H., Trushkyakov, V., Yutkin, E.: Tethered Tug for Large Low Earth Orbit Debris Removal. In: AAS Spaceflight Mechanics Meeting, January 29–February 2, Charleston, South Carolina, AAS 12-252 (2012)
8. Cougnet, C., Alary, D., Gerber, B., Utzmann, J., Wagner, A.: The debritor: an "off the shelf" based multimission vehicle for large space debris removal. In: 63rd International Astronautical Congress, 1–5 October 2012, Naples, Italy, IAC-12-A6.7.7 (2012)
9. Nishida, S., Kawamoto, S.: Strategy for capturing of a tumbling space debris. Acta Astronaut **68**, 113–120 (2011)
10. Lorenzini, E.C.: In-Space Transportation with Tethers, NASA Grant NAG8-1303. Final Report. Smithsonian Institution Astrophysical Observatory, Cambridge, Massachusetts (1999)
11. Aslanov, V.S., Ledkov, A.S.: Dynamics of the Tethered Satellite Systems. Woodhead Publishing Limited, Cambridge (2012)
12. Cartmell, M.P., McKenzie, D.J.: A review of space tether research. Prog. Aerosp. Sci. **44**, 1–21 (2008)
13. Barkow, B., Steindl, A., Troger, H., Wiedermann, G.: Various methods of controlling the deployment of a tethered satellite. J. Vib. Control **9**, 187–208 (2003)
14. Aslanov, V.S.: The effect of the elasticity of an orbital tether system on the oscillations of a satellite. J. Appl. Math. Mech. **74**, 416–424 (2010)
15. Aslanov, V.S., Yudintsev, V.V.: Dynamics of large debris connected to space tug by a tether. J. Guid. Control Dyn. **36**, 1654–1660 (2013). doi:10.2514/1.60976
16. Picone, J.M., Hedin, A.E., Drob, D.P., Aikin, A.C.: NRLMSISE-00 empirical model of the atmosphere[Text]: statistical comparisons and scientific issues. J. Geophys. Res. **107**(A12), 1–70 (2002), article number 1468
17. Regan, F.J.: Re-entry Vehicle Dynamics. AIAA, New York (1984)
18. Curti, H.D.: Gravity-gradient stabilization. In: Curti, H.D. (ed.) Orbital Mechanics for Engineering Students, pp. 530–543. Elsevier Butterworth-Heinemann, Oxford (2005)
19. Anderson, J.D.: Fundamentals of Aerodynamics. McGraw-Hill, New York (1984)
20. Jasper, L.E.Z., Seubert, C.R., Schaub, H., Trushkyakov, V., Yutkin, E.: Tethered tug for large low earth orbit debris removal. In: AAS/AIAA Astrodynamics Specialists Conference Astrodynamic Conference, January 29–February 2, Charleston, South Carolina, AAS 12-252 (2012)
21. Beletsky, V.V., Levin, E.M.: Dynamics of space tether systems. Adv. Astronaut. Sci. **83**, 1–500 (1993)
22. Wiggins, S.: Global Bifurcations and Chaos: Analytical Methods. Springer, New York (1988)